

Estimate of Geopressures using Conformal Mapping in Eccentric Wells

Uyara F. Silva, Manoel I. Q. Júnior, Santiago Lemos, Alan. F. Silva, Geovanne P. Furriel, Nikholas Segatti and Wesley P. Calixto

Abstract—The purpose of this work is to calculate Surge and Swab pressures in eccentric wells. Analysis of the phenomenon, in which fluid is confined between two eccentric cylinders, are made. Conformal mapping calculations is used to lead the original eccentric domain into equivalent concentric domain, since usual models only make calculation for concentric geometries. The results of this study, using the proposed methodology, are presented and discussed.

Index Terms— annulus geometry, conformal mapping, surge pressure, swab pressure, yield power law drilling fluid.

I. INTRODUCTION

The usual methodology for pressure calculation, during drilling of wells, assumes that the drill string and well work concentrically. However, the rotary movement of the drill makes the set (drill and well) works eccentrically with the well. Therefore, the calculations obtained through the usual methodologies have errors because they do not consider the effect of the eccentricity.

Surge and Swab pressures are problems that can happen during the drilling of oil wells [1]. The prediction of these pressures is essential to determine the appropriate speeds and accelerations for introduction and withdrawal of the drill string in the wellbore [2].

Surge pressure is the increase in wellbore pressure, that goes beyond the maximum supported by walls. It can fracture the rock formation and causes fluid loss [3]. Swab pressure occurs when pressure inside the wellbore is below the pore pressure, causing fluid penetration from the rock into the wellbore (kick effect). If not controlled, the kick effect can become blowout, which means uncontrolled flow from the hole to surface [2]. To avoid the blowout, it is necessary to control and to manage the pressures, ensuring that they are within desired limits [3].

Calculations of Surge and Swab pressures have extreme importance to avoid kick effect and subsequent blowout. Kick effect can occur when the hydrostatic pressure is lower than the pore pressure, fracturing the formation and thus the pore fluid invades the well. The absence of control of the kick effect can results in blowout, fluid inside the well reaches surface

uncontrollably and can cause explosions and dump of oil into the environment.

The usual methodology to calculate the Surge and Swab pressures assumes that the casing string and drill work concentrically [4]. However, the rotational movement of the drill causes the geometry of the well to be eccentric. Calculations obtained by usual methods do not consider the effect of eccentricity [5].

In order to reduce errors due to the eccentricity it can be used conformal mapping, that takes a domain into another, preserving the angles and physical quantities [6]. The purpose of this work is use conformal mapping to calculate the value of Surge and Swab pressures taking into account the effect of eccentricity between the casing string and the wellbore.

Conformal mapping are domain transformations and represent complex analytic functions, so this work assumes that conformal mapping are capable to lead eccentrics geometries into concentric geometries. Therefore, the value of the pressures can be calculated at any time of the drilling dynamics. The model is developed for power law drilling fluids under isothermal conditions, considering a constant fluid density. The model can be used in vertical wells, both terrestrial and marine. This work is focused on the problems caused by Surge and Swab pressures.

II. WELL DRILLING PROCESS

For drilling wells, the drill column with the drill in the tip is introduced into the formation, making the well [7]. The process of well drilling is made by steps, each step is drilled a given depth and thickness [8]. Introduction and withdrawing the drill string is called maneuver [9].

For each maneuver is introduced a new column set with new thickness down to a certain depth. During drilling, a hydrostatic fluid is injected through the drill bit into the well with the purpose of carrying gravels out of the wellbore. Hydrostatic fluid is also used to lubricate the drill bit and give more support to the wellbore walls. After drilling part of the well, the drill column is removed and then is introduced a casing string into the hole, a metal pipe used to support the wellbore wall which has just been bored, preventing landslides [10].

Surge pressure, Fig. 1 (a), occurs when the hydrostatic pressure of the fluid is above pores pressure at the time of introduction of the drill string with speed V_p

higher than adequate. Surge can also occur when drilling fluid is injected more than necessary, increasing pressure on the rock [11]. Hydrostatic pressure becomes greater than the fracture pressure (the rock strength) and can cause loss of drilling fluid. When this occurs, cementing of the well is required, to fill the space where the wellbore was fractured [12].

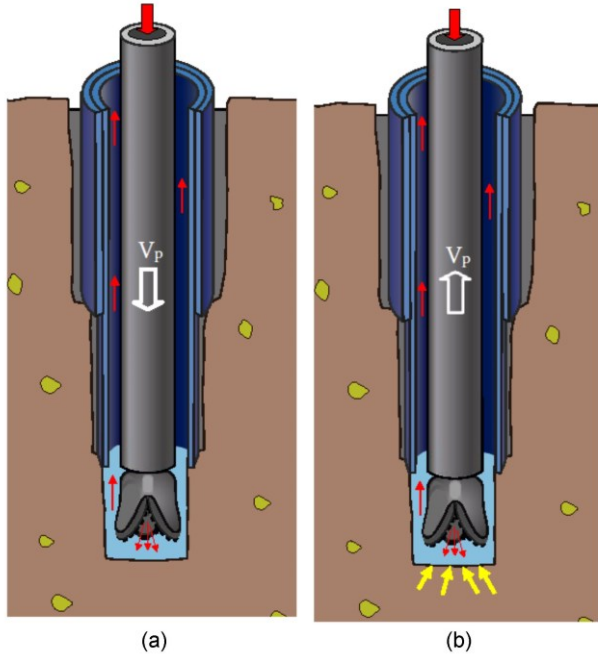


Fig. 1: Geopressures: (a) Surge and (b) Swab.

The Swab pressure, Fig. 1 (b), happens in the column withdrawal operation with speed V_p generating pressure drop by drag of the fluid along the tube walls [13]. When withdrawing the drill, vacuum can be generated causing hydrostatic pressure decrease, thus making pore pressure to become greater than hydrostatic pressure in the well and the kick effect to occur [12].

A. Pressures inside the well

The concept of pressure within wells is associated with the fluids contained within the rocks, and the result of the loading, which reacts equally in all directions.

1) *Pore pressure*: In rock formation, only part of the total volume is occupied by solid particles, which settle to form the structure. The remaining volume is often called voids, or pores, and is occupied by fluids. Pore pressure, often referred as formation pressure or static pressure, is the pressure of fluids contained in porous spaces of the rock. It is a function of the specific mass of the formation fluid and the loads it is bearing. In petroleum areas, the fluid filling a formation can be water, oil or gas [2].

2) *Hydrostatic pressure*: Hydrostatic pressure is exerted by the weight of the hydrostatic column of fluid,

being function of the height of the column and the specific mass of this fluid. The drilling fluid has as one of its main objectives to keep the well safe and stable. The pressure provided by the drilling fluid varies if it is inside the drill string or in the annulus. This difference occurs because when the fluid is returning through the annular space, it carry the dirty made by drilling process. The weight of suspended gravels increases the specific mass of the drilling fluid by providing higher pressure at the bottom of the well. Another variable that interferes with the hydrostatic pressure generated by the drilling fluid is that the fluid be static or moving [2].

B. Kick and Blowout Effects

The pressure inside the well must be between the minimum and maximum boundary (operating window), for this to occur, the amount of fluid injected into the well must be analyzed according to the structure of the formation. The operating window must be determined and respected during maneuvering to prevent the well wall from fracturing, by excessive hydrostatic pressure or by lack of weight to contain the pore pressure. The speed of the maneuver should also be well calculated before the introduction of the drill string.

According to the type of formation being drilled, the imbalance between the pressure inside the well and the pore pressure can have different consequences. If the pore pressure becomes larger than the pressure inside the well, the formation fluid may invade the well. This typical undesired occurrence is called kick and can lead to loss of time during drilling. If kick occurs, it should be controlled by a higher injection of hydrostatic fluid through the drill string. In more severe and uncontrolled cases, the kick may hit the surface, resulting in blowout, uncontrolled flow of fluid coming out of the well due to some failure in the pressure control system, which can have disastrous consequences such as total destruction of the platform and the death of workers or damage to the environment. On the other hand, pressures inside the well greater than the fracture pressure, resistance of the formation, can lead to the invasion of the well fluid to the formation, being possible the collapse of the well [2].

C. Operating window

The operating window determines the allowable pressure variation exerted by drilling fluid inside the well, in order to maintain the integrity of the well, respecting the pore, fracture and collapse pressures. This window should determine the minimum and maximum fluid weight that can be used inside the well. The operating window is used to prevent kick and blowout effects or landslide [2]. Fig. 2 illustrates an operating window example where the fluid weight limits should be between the fracture pressure and the pore pressure.

If the weight of the fluid is less than the pore pressure, there may be a kick effect, if the weight of the fluid is greater than the fracture pressure, there will be loss of fluid for formation and possible landslide [15].

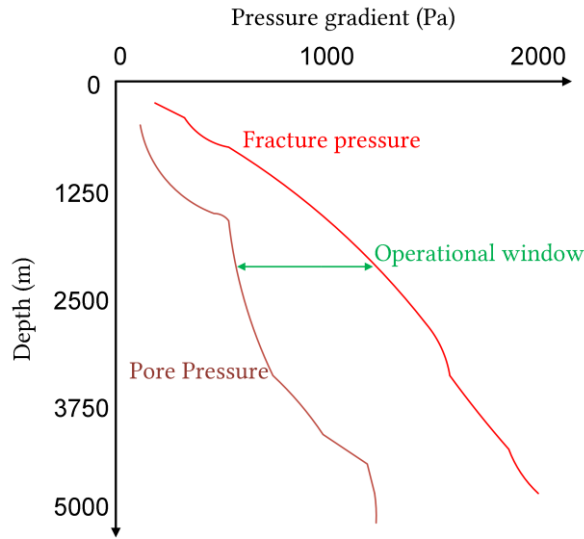


Fig. 2: Operational Window

III. CONFORMAL MAPPING

A deep-sea navigator can be guided by the stars and the angle that his course makes between the latitude and longitude lines. Since the Middle Ages, navigators have realized that it was possible to have spherical surface angles conserved on plane maps. When the angles between the curves on Earth are equal to the corresponding angles in the plane map, the map is called conform map [1].

The idea of a map conforming to the Earth was developed by the Belgian mathematician, geographer and cartographer Gerardo Mercator in 1569, known as Mercator projection. Although this projection presented distortions in proportions, it revolutionized cartography of the time. The points of the sphere, except the poles, are projected on a cylinder in which the sphere is inscribed, Fig. 3, the parallels are parallel straight horizontal lines, where the distance between successive parallels is proportional to their proximity to the Equator line, that is, the closer they are to the Equator, the smaller the distance between them. Meridians are projected in equidistant vertical parallel straight lines [1].

Advances in conforming map theory were performed by other scientists, Euler in 1777 (sphere in plan), and Lagrange in 1779 to obtain all the conforming representations of a part of the Earth's surface in a plane where all circles of longitudes and latitudes are represented by circular arcs in the plane. All of these authors, including Lambert with conforming conics, used complex numbers, but Lagrange's presentation is the clearest and most general.

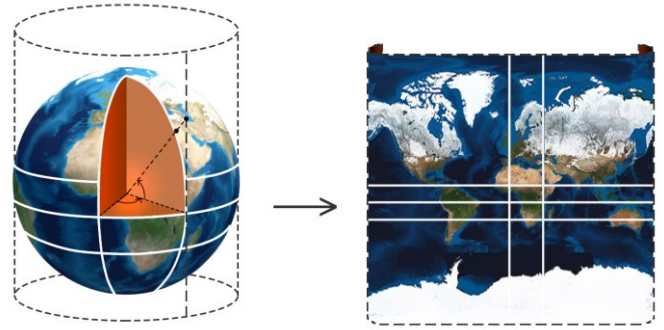


Fig. 3: Mercator Projection.

The discovery came in 1851 when Riemann gave the fundamental result, known as the Riemann's theorem, which was the starting point for all further developments in conformal mapping theory.

To prove this theorem, Riemann assumed that the variational problem, now known as the Dirichlet problem, has a solution. Fifty years later, in 1901, Hilbert demonstrated the existence of the solution of the Dirichlet problem. The validity of Riemann's result was rigorously established by Schwarz in 1890, using number of theorems coming from the logarithmic potential theory. At the end of the century XIX and the beginning of the century XX Cauchy, Riemann, Schwarz, Christoffel, Bieberbach, Carathéodory, Goursat, Koebe and others have established theoretical aspects about the theory of functions with complex variables

A. Conformal Mapping Definition

Conformal mapping are analytical functions, $w=f(z)$, that carry the points of the domain D in points of the domain I maintaining the property of the angles, capable of converting mathematical problem of difficult solution into a simpler one without changing the physical characteristics of the system. The function has domain and range in the complex plane. Under some restrictive conditions, the mapping function can be defined [6]:

$$w = f(x) = f(x + yi) = u(x; y) + v(x; y)i, \quad (1)$$

where

$$z = x + yi \quad (2)$$

and

$$v = u + vi. \quad (3)$$

Considering $w = f(z)$ the complex function that takes points from the plane z in points of the plane w , so $f(z)$ is a geometric transformation, since curves in the plane

z has as images, curves in the plane w . The curve C_0 in the complex plane z has the curve S_0 in the complex plane w as its image, Fig. 4.

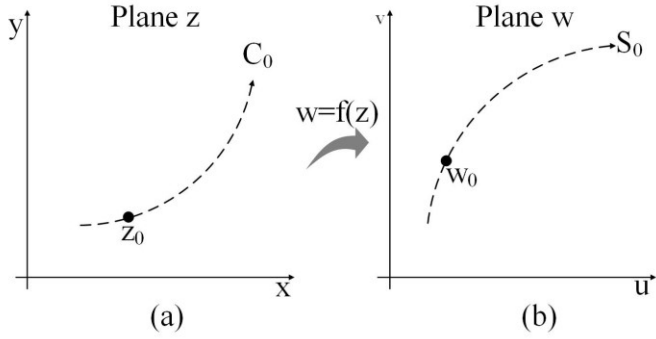


Fig. 4: Curve in z Plane and its Image in w Plane.

Considering positive direction of the course along C_0 , the corresponding positive direction over S_0 is determined by the transforming function f . Taking the point z_0 in C_0 , its image in w is $w_0 = f(z_0)$ over S_0 , as shown in Fig. 4. Considering also the $z_0 + \Delta z$ over C_0 in the positive sense from z_0 , the limit of the argument of Δz when it tends to zero is the angle of inclination α of the tangent line to C_0 in z_0 , Fig. 5 (a).

If $w_0 + \Delta w$ is the image of $z_0 + \Delta z$, then the argument of Δw tends towards the inclination angle β from the tangent to S_0 in w_0 , when Δw tends to zero, with orientation according to Fig.5 (b).

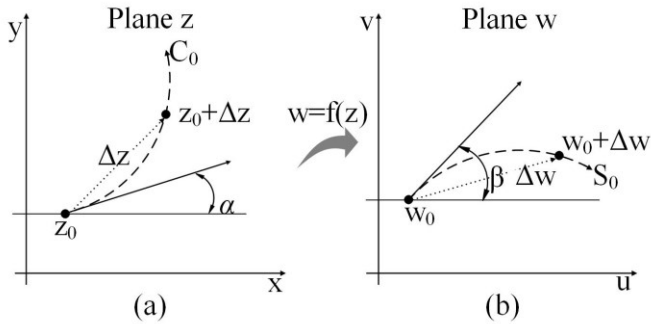


Fig. 5: Slope angle (a) α in Plane z and (b) β in Plane w .

IV. METHODOLOGY

A. Conformal Mapping

The problem in calculation of pressures consists in obtaining an equivalence between the eccentric and concentric plans. Fig. 6 illustrates the transverse section in the annulus formed between the wellbore and the column, by two coaxial cylinders with radii r_1 for external cylinder and r_2 for internal cylinder in the eccentric plane. The external plate is the well while inner plate is the column (drill).

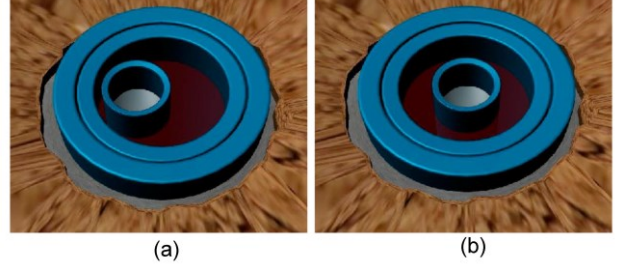


Fig. 6: Plan (a) eccentric in the domain D and plan (b) concentric in the domain I .

Assuming that the plates are circular in the total length and $\psi \neq 0$ is the eccentricity of the circles, there is in the Fig. 6 (a) the real problem. There is some difficulty to calculate the pressures in devices with this geometry. However, a new geometry that makes possible the pressures calculation can be found.

Using algebraic manipulation [14], it is possible to develop a conformal mapping, given by (4), that leads two eccentric circles with radii r_1 (external cylinder) and r_2 (internal cylinder) into two concentric circles Fig. 6 (b).

$$w(z) = t \cdot \frac{r_1}{r_2} e^{i\theta} \cdot \frac{d(z - z_a) - s(z_b - z_a)}{d(z - z_a) - t(z_b - z_a)}, \quad (4)$$

where θ , s and t are real, z_a are the points of the external plate and z_b , the points of the inner plate [6], s and t are the roots of the expression (4), given by:

$$\begin{aligned} s \cdot t &= r_1^2 \\ (d - s) \cdot (d - t) &= r_2^2. \end{aligned} \quad (5)$$

In (4), $d = |z_a - z_b| = \psi > 0$ and $z_a, z_b, r_1, r_2, R_1, R_2 > 0$ and $z_a \neq z_b$ [14], this equation can still write as:

$$\begin{aligned} \frac{r_2}{r_1} \cdot \frac{t}{(d - t)} &= \frac{R_2}{R_1}, \\ -\frac{-d^2 - r_1^2 + r_2^2 + \sqrt{-4d^2 r_1^2 + (d^2 + r_1^2 - r_2^2)^2}}{2d} &= t, \quad (6) \\ -\frac{-d^2 - r_1^2 + r_2^2 - \sqrt{-4d^2 r_1^2 + (d^2 + r_1^2 - r_2^2)^2}}{2d} &= s. \end{aligned}$$

Thus, in this new geometry, circles are concentric and the relationship between the domains D and I can be done.

B. Rheological Parameters

Fluids are classified according to their rheology, for this reason three parameters are considered: shear stress, shear rate and viscosity [15].

Shear stress τ is defined as the force F that, applied to an area A , the interface between the moving surface and

the liquid, causes flow in the first layer of liquid and the first layer causes flow in the second layer of liquid and so on. This moving surface is the drill string which moves when performing the maneuver.

Shear rate can be defined as variation of flow velocity with the variation of the distance between the drill string and walls of the well [15].

The viscosity is the ratio between shear stress and shear rate, and is the measure of the fluid resistance.

To calculate the shear stress over the shear rate in the well, the Hershell model is used. It is also known as Yield Power Law Fluid model, whose relationship of the three parameters is given by:

$$\tau = K\gamma^n + \tau_0, \quad (7)$$

where, τ is the shear stress and γ is the shear rate, τ_0 is the yield stress, K is the consistency index that indicates the degree of fluid resistance against the flow and n , named behavior index, indicates the distance of the Newtonian fluid model [15].

In the ratio $\gamma \times \tau$, for yield power law fluids, when the shear rate is $\gamma = 0$, the shear stress is the yield stress τ_0 . The yield stress is the minimum stress necessary for the fluid to start leaking [15].

C. Mathematical Model for Surge and Swab Calculation

In order to determine Surge and Swab pressure in concentric plan is necessary to determine the input values for the annular geometry and the rheology of the fluid used in the drilling of the well.

For the rheology of the fluid, there are considered three parameters: shear stress, shear rate and viscosity. The shear stress τ is defined as the force F that, applied on an area A of the interface between the moving surface and the liquid, causes flowing in the first liquid layer, which in turn causes, in the second, the second in the third, and so on.

This moving surface is the drill string which moves during the performing maneuver. Shear rate can be defined as variation in flow rate with the height variation (distance from the surface causing the shear) [15].

The viscosity is the ratio between shear stress and shear rate, and is a measure of resistance to fluid flow.

The annular geometry, Fig. 7, is the height H , which is the distance between the surface of the drill string and the well, the diameter of the well $d_h = 2R_1$, the diameter of the drill string $d_p = 2R_2$, and the velocity V_p of descent or ascent of the drill string. Since the used methodology for calculating the pressures considers the concentricity between the well and the drill string, $H=R_1 - R_2$.

The rheological parameters are: the consistency index K , the fluid behavior index n and the initial shear

stress required for the flow called yield stress τ_0 [12].

The values of Surge and Swab pressure are calculated by [3]:

$$P_{su} = \frac{P_e^n}{\left(\frac{n}{n+1}\right)^n \left(\frac{H}{V_p}\right)^n \left(\frac{H}{K}\right)} \cdot L, \quad (8)$$

where L is the total length of the drill string and P_e is the specific pressure obtained from the ratio of the well geometry and the rheological parameters of the fluid.

The difference between Surge and Swab is that the Surge is the increased pressure on the well when the drill string down, and the Swab is the decrease of pressure in the well when the drill column rises.

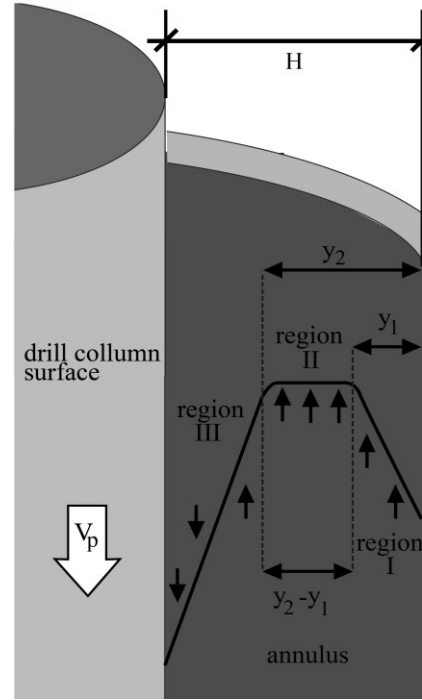


Fig. 7: Annulus geometry.

For the calculation of (8) is necessary to find expressions that define the speeds in the three regions of Fig. 7. The model for calculating the speed was developed by Crespo and Ahmed [12], for yield power law fluids.

Vector y assumes values between 0 and H , and is given in meters. For each value of y , there is a value for the velocity of the flow, indicated by the vertical arrows.

The constant y_1 is the size of region I and y_2 is the sum of region I and region II. Region II is within the limits $y_1 \leq y \leq y_2$ and has constant speed, the region I is within the limits $0 \leq y \leq y_1$ and region III is within the limits $y_2 \leq y \leq H$. The velocities in the region I and in the region III

vary according to vector y [12].

For the velocity profiles in the regions of the mathematical model of Crespo, dimensionless variables for speed are used as (9):

$$V'_i = \frac{V_i}{V_p}, i = 1, 2, 3. \quad (9)$$

This variables are dimensionless because of the division between two quantities with the same unit of measurement.

The same is true for the values of widths y_1 and y_2 , as (10):

$$y'_i = \frac{y_i}{H}, i = 1, 2. \quad (10)$$

Values of y'_i , are always between 0 and 1 because they are the results of the divisions between points in y and their maximum value, H . So, these values are dimensionless.

The velocity profile in the region I is given by:

$$V'_1 = P[(y'_1 - y')^b - (y'_1)^b], \quad (11)$$

where $0 \leq y' \leq y'_1$.

The velocity profile in the region II is given by:

$$V'_2 = 1 - P(1 - y'_2)^b, \quad (12)$$

where $y'_1 \leq y' \leq y'_2$.

The velocity profile in the region III is given by:

$$V'_3 = 1 - P[(1 - y'_2)^b - (y' - y'_2)^b], \quad (13)$$

where $y'_2 \leq y' \leq 1$.

The values y'_1 and y'_2 are the widths shown in Fig. 7 and are associated with regions of different velocity profiles of fluid. The exponent b used in (11), (12) and (13) takes account the fluid behavior index:

In (11), (12) and (13) the value of the dimensionless pressure P is given by:

$$P = \left(\frac{n}{n+1}\right) \left(\frac{H}{V_p}\right) \left(\frac{\Delta P H}{L K}\right)^{1/n}. \quad (14)$$

Expression (12) is related to the pressure variation ΔP in the total length L of the drill string, P is a dimensionless vector.

The total flow rate is the sum of the flow rate of the three regions given by [3]:

$$q'_t = \int \left(\int V'_1 dy'_1 + \int V'_2 dy'_1 + \int V'_3 dy'_1 \right) dx'. \quad (15)$$

Solving the integral in (15), is obtained:

$$q'_t = -P \left[\left(\frac{b}{b+1} \right) y_1'^{b+1} \right] - [P(1 - y'_1 - \chi)^b - 1] (1 - y'_1 - \chi) + P \left(\frac{b}{b+1} \right) (1 - y'_1 - \chi)^{b+1} - P y'_1 \chi \quad (16)$$

Where:

$$\chi = \frac{2\tau_0}{\frac{H}{\Delta P} \frac{L}}{L} \quad (17)$$

and

$$(1 - y'_1 - \chi)^b - (y'_1)^b - \frac{1}{P} = 0. \quad (18)$$

In (18), the value of y'_1 is obtained by iteration by Newton-Raphson method.

Relating the geometry of the well and the drill string (geometry of the annulus), it is possible to calculate the specific flow rate using [3]:

$$q'_e = \frac{-1}{\left(\frac{R_1}{R_2}\right)^2 - 1}. \quad (19)$$

Reconnecting the rheology of the fluid with the geometry of the annular space ($P \times q'_t$), the interpolating polynomial is obtained:

$$f(q'_t) = P_e. \quad (20)$$

With interpolating polynomial (20) and (19), is possible to find the value of P for the value of $q'_t = q'_e$, that is, $P(q'_e)$.

P_e is the specific pressure that will be used in (8).

The variables V'_1 , V'_2 , V'_3 , y' , y'_1 , y'_2 , y'_3 and q'_t are dimensionless.

D. Algorithm

To obtain the values of P_{su} the following algorithm is used: i) The bilinear transformation given by the expression (4) is used to obtain the equivalent concentric plane and thus the constant value of H is obtained; ii) with the input parameters, rheological and geometric, the value of P is obtained from (14), for each given value of ΔP ; iii) with P , the value of y_1 in (18) is calculated for the combination of the input values ΔP and V_p ; iv) the value of y_1 is replaced in (16), so, the value of the total flow q_t is obtained for each value of L ; v) soon, q_e is obtained from (19); vi) The graph relating P and q_t is generated, it presents the relation between the geometry of the annular space and the rheology of the fluid. This graph represents the relation between the geometry of the annular space and the rheology of the fluid. From this relation the interpolating polynomial is created (20) and the value of P_e is obtained, (q_e, P_e) is the point on the graph (q_t, P) and vii) with the value of P_e the values of the pressures Surge and Swab, P_{su} , can be obtained using (4). The Fig. 8 shows the flowchart produced.

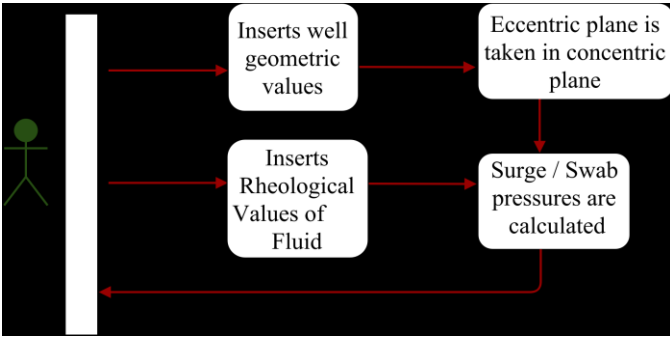


Fig. 8: Algorithm.

V. RESULTS

As results, it is presented the calculation of the Surge pressure in a dummy well using the usual methodology and the proposed methodology. A comparison was made between the values obtained for each methodology. A study was performed on the relationship between eccentricity and pressures values. The maximum eccentricity for the well geometry was calculated.

A. Case Study 1: Eccentricity \times Geopressions

To relate the eccentricity to the geopressures it is necessary to have the input parameters. However, the thickness H , in the usual models is not uniform throughout the circumference of the coating column (there is eccentricity). In this way, it is proposed that the drilling of the well be monitored, and at each interval of time Δt , determined by the user, the concentric geometry equivalent is obtained.

All case studies use data from Crespo, which are: i)

geometry, considering the well being drilled by drilling column with length $L=36$ m, diameter $d_2=0.254$ m and diameter of the coating column $d_1=0.508$ m and ii) rheological, yield power law fluid with $n=0.48$, $K = 0.74$ Pa.sⁿ e $\tau_0 = 3.11$ N/m².

1) *Calculation of Geopressure Considering Traditional Methodology*: In order to carry out this case study, it is considered the drilling of the well whose radius of the coating column and the radius of the drilling column form concentric geometry. For calculation of the Surge pressure, generated in the descent of the column with constant speed $V_p=0.1524$ m.s⁻¹, the usual methodology ignores the value of eccentricity. Then the thickness H of the annular space is only the subtraction of the radius of the coating column by the radius of the drilling column $H = r_1 - r_2 = 0.127$ m.

Assuming, for all studies, $\Delta P = 1.38 \times 10^7$ Pa, equivalent to 2000 psi at the bottom of the well, it is possible to obtain the vector P using (14), relating well geometry to fluid rheology. With vector P , it is possible to obtain the vector of the flow rate q_t .

Using (19), it is possible to obtain $q_e = -0.33$ and having the interpolating polynomial (20), it is possible to obtain $P_e = 3.68$. Substituting the P_e value in (4), obtains the Surge pressure value, $P_{su} = 1.84 \times 10^5$ Pa, equivalent to 26,78 psi.

In the real well drilling system, the drill string and casing column do not work concentrically. If there is a maximum eccentricity, when the drill string abuts the casing column, they can stick together, damaging drilling the well.

TABLE I provides the input and output values for the usual model, which does not consider the value of the eccentricity in the calculations.

TABLE I
RESULT CONSIDERING THE USUAL METHODOLOGY

Symbol	Quantity	Value
ψ	eccentricity	0.1257 m
n	behavior index	0.48
K	consistency index	0.74 Pa.s ⁿ
τ_0	yield stress	3.11 N/m ²
r_1	radius of the coating column	0.254 m
r_2	radius of the drilling column	0.127m
P_{su}	Surge	1.84×10^5 Pa

2) *Calculation of Geopressure with Eccentric Geometry*: To use the geometry of the previous case considering the eccentricity, before using the mathematical model of Crespo, the equivalent concentric geometry must be calculated. The values of R_1 e R_2 of the concentric

plane, are the new rays of the coating column and drilling column, respectively. As the conformal mapping do not change the magnitudes of the system, the values of ΔP remain the same for both eccentric and concentric geometry.

For the geometry under study, there is maximum eccentricity $\psi_{\max} = 0.1257$ m. From this eccentricity, the value of the Surge geopressure can be calculated using the conformal mapping in (4), Which carries the eccentric plane of Fig. 9 (a) in the concentric plane of Fig. 9 (b). The new radius of the concentric plane are $R_1 = 0.2806$ m for coating column and $R_{2m} = 0.2539$ m for drill string. From this conformal mapping $H = 0.0267$ m is obtained.

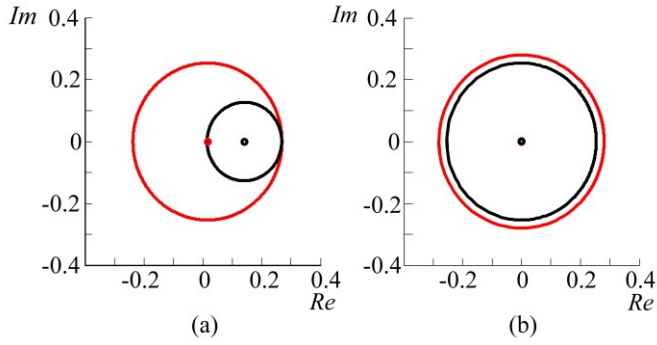


Fig. 9: Real System Transformation (a) Eccentric Plane e (b) Concentric Plane.

Applying the calculations of the mathematical model of the annular space in the new concentric plane, Fig. 9 (b), it is possible to get the value of Surge geopressure of 1.56×10^6 Pa, equivalent to 226.63 psi.

Using the usual methodology, the value of $P_{su} = 1.84 \times 10^5$ Pa or $P_{su} = 26.78$ psi. Using the proposed methodology and taking into account the eccentricity, it is possible to obtain the value of $P_{su} = 226.63$ psi. The proposed methodology finds, in this case, a value of approximately 8.46 times higher than the value found by the traditional methodology. A fact that occurs by not considering the eccentricity, which could cause serious problems at the moment of the maneuver.

The TABLE II provides the input and output values for the case study considering the eccentricity and using the proposed methodology.

Symbol	Quantity	Value
ψ	eccentricity	0.1257 m
n	behavior index	0.48
K	consistency index	0.74 Pa.s ⁿ
τ_0	yield stress	3.11 N/m ²
r_1	radius of the coating column	0.254 m
r_2	radius of the drilling column	0.127 m
R_1	radius of the coating column after conformal mapping	0.2806 m
R_2	radius of the drilling column after conformal mapping	0.2539 m
P_{su}	Surge	1.56×10^6 Pa

Considering the same input parameters, but with $\psi = 0.062$ m, the new geometry is calculated. The equivalent concentric plane, has $R_1 = 0.4664$ m and $R_2 = 0.2539$ m for the coating column and the drilling column, respectively, as illustrated in Fig. 10.

Applying the calculations of the mathematical model in the new concentric plane, Fig. 10 (b), it is possible to reach the value of $P_{su} = 8.642 \times 10^4$ Pa equivalent to $P_{su} = 12.51$ psi.

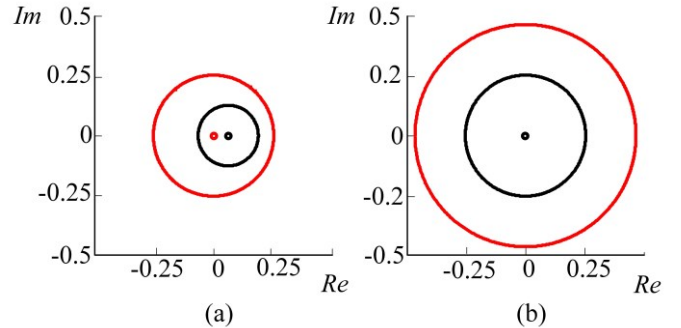


Fig. 10: Real System Transformation (a) Eccentric Plane and (b) Concentric Plane.

This result shows the dynamics of the effect of the eccentricity on the pressures at the bottom of the wells, since all the configurations were maintained, varying only the eccentricity. For average eccentricity, $P_{su} = 12.51$ psi, 2.14 times lower than the value obtained using the traditional methodology.

The TABLE III provides the input and output values for the case study with $\psi = 0.062$ m and considering the eccentricity and using the proposed methodology.

TABLE III
RESULT CONSIDERING CONSTANT ECCENTRICITY

Symbol	Quantity	Value
ψ	eccentricity	0.062 m
n	behavior index	0.48
K	consistency index	0.74 Pa.s ⁿ
τ_0	yield stress	3.11 N/m ²
r_1	radius of the coating column	0.254 m
r_2	radius of the drilling column	0.127 m
R_1	radius of the coating column after conformal mapping	0.4664 m
R_2	radius of the drilling column after conformal mapping	0.2539 m
P_{su}	Surge	8.642×10^4 Pa

B. Case Study 2: Calculation of Geopressures with Variation in Eccentricity

Considering also the situation in which the rotary movement of the drill descending into the well causes the drill string and the casing column to generate different eccentric geometries for each depth, that is, ψ is different for each value of $\Delta P/\Delta L$, it is possible to calculate the Surge geopressure in each section of the well. In this case, it is also considered the speed of descent varying in time, speed increases with depth. For this case it varies from $V_p = 0$ to $V_p = 0.1524$ m.s⁻¹.

For this case, the pressure ΔP varies from $\Delta P = 1.37 \times 10^6$ Pa, on the surface until $\Delta P = 1.38 \times 10^7$ Pa, at the well bottom.

It is observed that there is variation in the value of the eccentricity because the system is dynamic, and the eccentricity varies in time, so it is possible, using the conformal mapping and considering the variation of the eccentricity $0 < \psi < 0.1257$ m, calculate the new H values for the eccentricity vector.

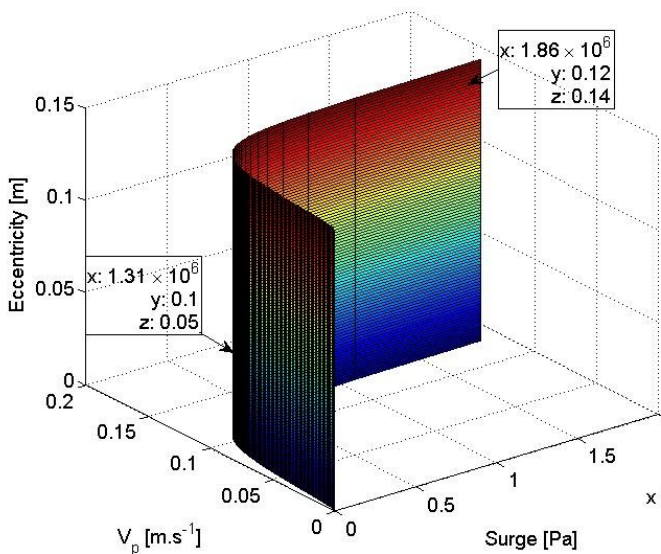


Fig. 11: $P_{su} \times V_p \times \psi$

It is possible to produce the surface that relates the eccentricity, the Surge geopressure and the descent speed of the drill, as shown in Fig. 11.

It is observed in Fig. 11, that higher the descent speed V_p , greater the increase in surge pressure, in this case it would be feasible to establish the maximum velocity of 0.1 m/s, from this point Surge pressure begins to grow exponentially. In the same way, another surface can be produced that relates ψ , Surge and ΔP , as shown in Fig. 12.

Fig. 12 shows that the higher the pressure ΔP inside the well, the higher the Surge pressure. Fig. 12 indicates whether the injected fluid levels are suitable for well geometry.

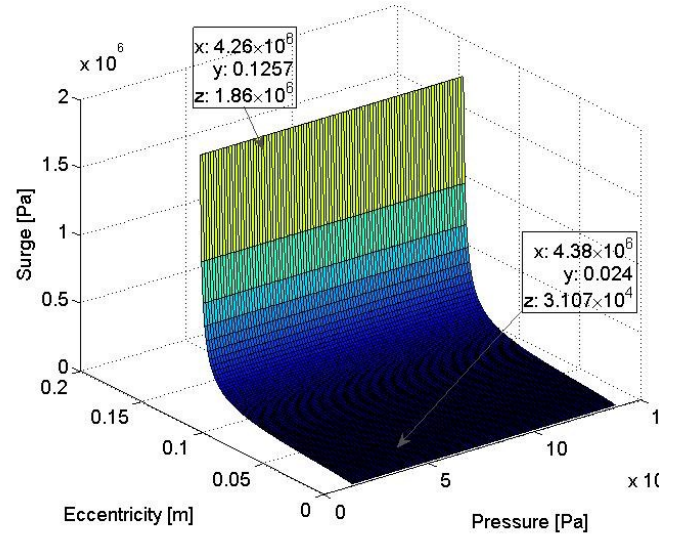


Fig. 12: $\psi \times \Delta P \times P_{su}$

The traditional method and the proposed method start from the same point when there is concentricity. However, for the input data presented (geometry and rheology) and considering variations in eccentricity values and ΔP , it can be observed that the values of Surge for the traditional method are higher than for the proposed method until a certain value. Fig. 13 illustrates the comparison between the traditional method and the proposed method, which considers eccentricity.

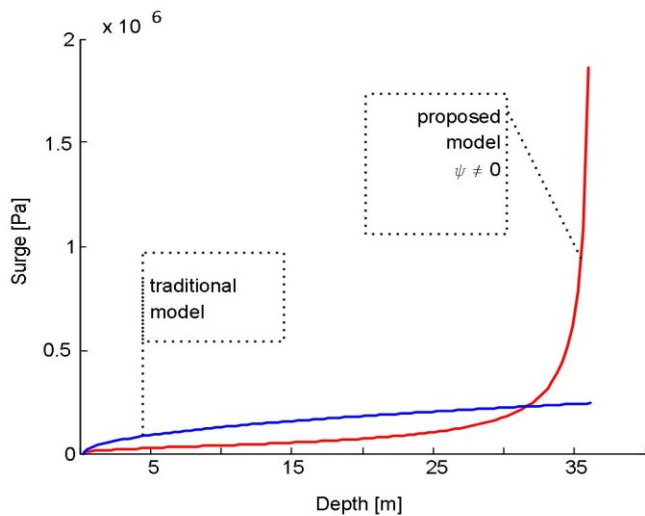


Fig. 13: Comparison between Surge Values Obtained

If the value of Surge pressure is greater than the real one, can cause damage to the formation, therefore, the operating window that contains the pressures and speeds, ideal for safe operation of the maneuvers, has maximum and minimum boundary. If the calculated pressure value is incorrect, hydrostatic fluid will be injected erroneously. The pore pressure may be greater than the rock fracture pressure, and may cause the kick effect. Therefore, it is important to know the operating window, the velocity values that the well supports and the actual geopressure values.

VI. CONCLUSIONS

It is possible to observe that the eccentricity produces incoherence between the adopted model and the real system. With the proposed methodology it is possible to calculate the maximum and minimum pressures, related to the maximum and minimum eccentricities that alter the values of H in the well drilling. The flow depends on pressure range, length of the drill string, well and drill string radius. In turbulent flows the speed of the drilling column and hydrostatic fluid is of great importance for the calculation of the variation of pressure in the bottom of the well. Pressure change increases exponentially with increasing drilling column speed. The increase in pressure also depends on the depth of the well. Pressure variation also depends on annular space, flow rate increases with increasing thickness H . To reduce pressure changes it is important to monitor speed and eccentricity between columns as well as amount of hydrostatic fluid injected into the well. The proposed method is able to calculate the Surge and Swab geopressures for non Newtonian fluids at the bottom of the well, considering the variation of the eccentricity of the same.

- [1] U. F. Silva, M. I. Q. Júnior, G. P. Furriel, A. H. F. Silva, A. J. Alves, and W. P. Calixto, "Application of conformal mapping in the calculation of geological pressures," Chilecon, 2015.
- [2] L. A. S. Rocha and C. T. Azevedo, Geopressures and Settlement Coatings columns (in Portuguese); 2 edition. Interciência, 2009.
- [3] F. Crespo and R. Ahmed, Experimental Study and Modeling of Surge and Swab Pressures for Yield-power-law Drilling Fluids. PhD thesis, University of Oklahoma, 2011.
- [4] O. N. Mbee, "Prediction of surge and swab pressure profile for flow of yield power law drilling fluid model through eccentric annuli," Master's thesis, African University of Science and Technology, 2013.
- [5] Z. Bing, Z. Kaiji, and Z. Ginghua, "Theoretical study of steady-state surge and swab pressure in eccentric annulus [j]," Journal of Southwest - China Petroleum Institute, vol. 1, 1995.
- [6] W. Calixto, "Application mapping as at the carter factor calculation (in portuguese)," Master's thesis, Federal University of Goias, 2008.
- [7] W. F. Rogers, "Compostion and properties of oil well drilling fluids, "Gulf Publishing Co., Houston, TX, 1948.
- [8] W. C. Frison, "Apparatus and method for treatment of wells," May 9 1989. US Patent 4,828,033.
- [9] D. Amorim Júnior and W. Iramina, "Maneuvers for exchanging drills in oil wells (in portuguese)," *TN Petróleo*, vol. 61, pp. 190–194, 2008.
- [10] R. Caenn and G. R. Gray, "Drilling fluid and completion; 6 edition (in portuguese)," Editora Elsevier, pp. 1–5, 2014.
- [11] A. G. Karlsen, "Surge and swab pressure calculation: Calculation of surge and swab pressure changes in laminar and turbulent flow while circulating mud and pumping," Institutt for petroleumsteknologi og anvendt geofysikk, 2014.
- [12] F. Crespo and R. Ahmed, "A simplified surge and swab pressure model for yield power law fluids," Journal of Petroleum Science and Engineering, vol. 101, pp. 12–20, 2013.
- [13] W. P. Calixto, B. Alvarenga, J. C. da Mota, L. d. C. Brito, M. Wu, A. J. Alves, L. M. Neto, and C. F. Antunes, "Electromagnetic problems solvng by conformal mapping: A mathematical operator for optimization (in portuguese)," Mathematical Problems in Engineering, 2011.
- [14] H. Kober, Dictionary of Conformal Representations, vol. 2. Dover New York, 1957.
- [15] J. C. V. Machado, Rheology and Fluid Flow - Emphasis on Oil Industry (in Portuguese); 2 edition. Editora Interciência, 2002.